THE UNIVERSITY of EDINBURGH

# Edinburgh Research Explorer

# -Chitin nano-Fibrils Self-Assembly in Aqueous Environments

**Link:**
Link to publication record in Edinburgh Research Explorer

**Document Version:**
Peer reviewed version

**Published In:**
Biomacromolecules

OPEN ACCESS

1 # β-Chitin nano-Fibrils Self-Assembly in Aqueous

2 # Environments

3 *Devis Montroni [1], Bartosz Marzec [2†], Francesco Valle [3,4], Fabio Nudelman [2]\*, and Giuseppe*

4 *Falini [1]\**

5 [1] Dipartimento di Chimica "G. Ciamician", Alma Mater Studiorum − Università di Bologna, via

6 F. Selmi 2, 40126 Bologna, Italy.

7 [2] EaStCHEM School of Chemistry, University of Edinburgh, David Brewster Road, Edinburgh,

8 EH9 3FJ, UK.

9 [3] National Research Council (CNR), Institute for Nanostructured Materials (ISMN), Via P. Gobetti

10 101, 40129 Bologna, Italy.

11 [4] Consorzio Interuniversitario per lo Sviluppo dei Sistemi a Grande Interfase (CSGI), ISMN-CNR,

12 40129 Bologna, Italy.

14

15

16

1    ABSTRACT. Chitin is one of the most studied biopolymers but the understanding of how it

2    assembles from molecules to micro-fibers is still limited. Organisms are able to assemble chitin

3    with precise control over polymorphism, texture, and final morphology. The produced hierarchical

4    structure leads to materials with outstanding mechanical properties. In this study the self-assembly

5    in aqueous solutions of β-chitin nano-fibrils, as far as possible similar to their native state, is

6    investigated. These nano-fibrils increase their tendency to self-assemble in fibers, up to millimetric

7    length and ≈10 μm thickness, with the pH increasing from 3 to 8, forming loosely organized

8    bundles as observed using cryo-TEM. The knowledge from this study contributes to the

9    understanding of the self-assembly process that follows chitin once extruded from cells in living

10   organisms. Moreover, it describes a model system which can be used to investigate how other

11   biomolecules can affect the self-assembly of chitin nano-fibrils.

# 1 Introduction

2 Chitin is the second most abundant natural biopolymer on earth[1] and the most common one in the

3 animal and fungi kingdoms. It has been found in arthropods, fungi, mollusks, etc.[2,3] where it has

4 been used for either protective, or structural purposes. Similarly to other structurally-related

5 materials, such as cellulose,[4] chitin forms different polymorphs: α-chitin, β-chitin, and γ-chitin[5],

6 whereby α-chitin, which is often found in arthropods,[2] is the most common and abundant. α-chitin

7 is characterized by an antiparallel packing of chains, leading to a strong network of hydrogen

8 bonds.[6,7,8] In contrast, polymeric chains within β-chitin, which is typical for mollusks[9,10] and

9 foraminifera,[11,12] display a parallel orientation. This polymorph presents a weaker network of

10 hydrogen interactions and a more opened structure when compared to the previous one.[1,4,8] Finally,

11 γ-chitin presents two chains arranged in parallel and one in antiparallel direction. This polymorph,

12 however, is uncommon in nature.[5,13]

13 Biogenic chitin, as well as other biopolymers,[14,15,16,17] displays remarkable levels of

14 organization[9,18,19,20,21,22,23] that contribute to its material properties. Many studies aiming to

15 synthetically replicate its structure and properties have been carried out.[24,25,26,27] Despite all those

16 attempts, natural chitin structures still outperform their synthetic analogues in many fields, as in

17 mechanical performances,[28] or controlling crystal precipitation.[29] The different properties between

18 the two chitins originates mainly from the precisely controlled hierarchical organization observed

19 in the natural material, as opposed to synthetic ones. In other fields, such as optics, bioinspired

20 chitin structures outperformed their natural analogues, but in this case different materials were

21 used.[30]

22 The chitin biogenesis process has not been completely understood.[31] Most studies have been

23 focused on fungi,[32] because of their fast growth and abundance. The process has been observed to

take place in three steps: i) the enzymatic synthesis of the polymer at the cytoplasmic-chitosome interface, ii) the translocation of the growing polymer across the membrane and its release into the extracellular space, and iii) its self-assembly to form crystalline micro-fibers combining with other sugars, proteins, glycoproteins, and proteoglycans until reaching a final structure.[33] Although many studies targeted the chitin synthase in insects,[34] the route leading to complex structures, such as arthropods' exoskeletons, or wings, remains unexplored. Similarly, while a chitin synthase involved in shell formation was recently identified in mollusks, its biosynthetic pathway and how it leads to complex 3D architectures are still unknown.[35,36] In calcifying organisms the 3D architecture of β-chitin fibers is specific to each mineralized tissue, and understanding its self-organization represents an important scientific challenge. This specificity demonstrates the tight control that the mineral-forming cells exert over the assembly, and spatial organization of chitin at all hierarchy levels. Looking beyond the self-assembly process, the supramolecular organization of chitin is a crucial factor affecting the formation of inorganic phases, providing polymorph selection, influencing crystal texture, and – importantly - controlling the morphology of growing particles.[37,38]

In this study we investigated the mechanism of β-chitin nano-fibrils assembly into micro-fibers in an aqueous solution. β-chitin was selected instead of the more common α-chitin for two main reasons: i) its more opened and hydrated structure could be more easily dispersed in water, and ii) it could convert to α-chitin enabling us to study the best conditions for this phase transition.

Chitin self-assembly is a biologically-relevant process, and its understanding will also help to describe the assembly mechanisms of other polysaccharide-based biopolymers that form highly ordered structures, such as cellulose. It will lead to new studies aiming to develop methods facilitating the production of highly organized fibrous biomaterials from cheap sources, and the

1 development of bionic approaches to biopolymers. Since this particular biopolymer is also present

2 in pathogens, such as fungi and pests, understanding the mechanisms of its supramolecular

3 assembly can help with the development of new drugs targeting that process.

4

## 5 Materials and methods

### 6 Materials

7 All reagents and solvents were purchased from Sigma Aldrich and utilized without any further

8 purification. Squid pens from *Loligo vulgaris* were collected from a local market. Once hydrated,

9 the lateral blades were isolated, cleaned with distilled water and ethanol 70 vol.%, and then stored

10 dry.

### 11 Squid pen de-proteination

12 The β-chitin from the squid pen was purified from proteins by soaking about 1 g of the previously

13 washed squid pens in 100 mL of a pH 2 HCl solution (10 mM) containing 20 mg of pepsin (an

14 aspartic protease that breaks down proteins into smaller peptides).[39] The solution was placed on a

15 rocking table for 24 hours at 37 °C. After this first de-proteination, the squid pens were collected

16 and washed carefully with distilled water. The wet squid pens were then re-immersed in 100 mL

17 of a 100 mM phosphate buffer solution at pH 7.6 containing 20 mg of trypsin (a serine protease

18 that hydrolyzes proteins).[40] As in the previous step, the solution was placed on a rocking table at

19 37 °C for 24 hours. The removal of proteins from the pen was evaluated by the disappearance of

20 UV absorption peaks originating from tryptophan residues and observed at 280 nm using a Varian

21 Cary 300 Bio spectrophotometer.

**β-Chitin nano-fibrils (β-CnFs) preparation**

A homogeneous dispersion of β-chitin nano-fibrils (β-CnFs) was obtained by placing 50 or 100 mg of protein-free β-chitin, cut into about 0.5 cm$^2$ square pieces, in 100 mL of an acetic acid solution at pH 3 (5.6 mM).[41] The solution was stirred vigorously for 72 hours at room temperature. At the end of the process, a dispersion of CnFs was obtained. The dispersion was transparent, stable (for over 6 months), homogeneous, and highly viscous.

**β-CnFs self-assembly**

β-CnFs self-assembly was induced by changing the pH of 5 mL of freshly prepared (less than 24 hours from preparation) β-CnFs dispersion. The pH change was induced using NaOH 1 M and measured using a pH-meter BASIC 20 (pH ± 0.01) by Crison Instruments coupled with a HI1048 pH electrode (Hanna Instruments). The pH-meter was calibrated daily. The solutions were left for 24 hours at room temperature (25 °C) without any stirring. The morphological analysis were performed without any further purification of the mixture. For structural analysis the samples assembled were frozen with liquid nitrogen and lyophilized using a FreeZone® 1 (Labconco Corp., Kansas City, MO, US). The obtained material was then dispersed in 10 mL of Pre-milliQ water and centrifuged at 2000 g for 5 minutes. After that time the solution was disposed and the process was repeated two more times. Finally, the fibers were lyophilized for the last time upon freezing with liquid nitrogen.

**β-CnFs self-assembly kinetics**

The self-assembly of β-CnFs was investigated as a function of time in a 0.5 mg mL$^{-1}$ β-CnFs dispersions. 45 mL of freshly prepared dispersion (always less than 24 hours from preparation) were adjusted to different pH values in a test tube. At any reported time the solution was mildly

stirred and 5 mL of dispersion were isolated, observed with an optical microscope, frozen using liquid nitrogen, and lyophilized. The obtained material was dispersed in 10 mL of Pre-milliQ water and centrifuged at 2000 g for 5 minutes, after that the solvent was disposed and the process repeated two more times. Finally, the fibers were lyophilized again upon freezing with liquid nitrogen.

**Optical microscopy observations**

Optical microscopy images were collected using a SM-LUX POL microscope equipped with a Miticam 5 5.0 MP camera. Right after the end of the assembly process the sample was stirred, a drop of sample was collected and placed on a microscope slide, covered with a cover slip, and observed immediately.

Cross-polarized light images were used to carry out the fibers area unit coverage analysis. All images were collected using the same gain and exposition time. Each sample was screened to record a complete map of the glass slide and 12 images with no common areas, and with the higher surface covered were analyzed. Optical microscopy images were processed using Gwyddion, an open access software originally developed for the analysis of Scanning Probe Microscopy images but here used to have a quantitative evaluation of the material adsorbed onto the surface. Briefly, the chitin fibers present on the surface were detected by setting an intensity threshold (constant throughout all the images) and then the coverage was measured as the ratio between the covered and the total area.

**Electron and Probe Microscopy imaging**

Samples for AFM imaging were prepared by depositing 10 µL of the chitin material from the 0.5 mg·mL$^{-1}$ β-CnFs dispersion on a mica surface and gently drying them with a nitrogen flow.[42] The

AFM used was an AFM Multimode VIII controlled by the Nanoscope V electronic software package (Bruker, Santa Barbara, CA, US). The microscope was operated in the ScanAsyst mode and the cantilevers were ScanAsyst with an elastic constant of 0.40 N m$^{-1}$. The length and height of the nano-fibrils were measured by analyzing AFM images with Gwyddion. The fibrils present on the surface were isolated from the background by selecting an appropriate threshold, and the height was measured as the maximum height with respect to the sample surface. The length was measured as the end-to-end distance. Considering that fibrils' persistence length was longer than their actual length this value was a good approximation of their contour length.

Cryo-TEM imaging was carried out using a FEI Tecnai F20 transmission electron microscope equipped with a Schottky field emission gun and operated at 200 keV. For sample preparation, cryo-TEM grids (R2/2 200 µm mesh Au/C, Quantifoil Micro Tools Gmbh) were plasma-treated using a Quorumtech Q150T Glow Discharge system for 45 seconds. Aliquots of 3 µl of the aqueous mixture containing the fibrils/fibers, right after the assembly time considered, were applied to the cryo-TEM grids. Samples were then vitrified in liquid ethane using the FEI Vitrobot (Mk IV) plunge freezer and loaded to a Gatan cryo-holder cooled to 77 K with liquid nitrogen. Images were recorded on an 8k x 8k CMOS TVIPS F816 camera.

**Structural analysis**

Fourier-transform infrared spectroscopy (FTIR) spectra were collected using a Nicolet IS10 spectrophotometer. Omnic software (Thermo Electron Corp., Woburn, MA) was used for data processing and baseline correction. The samples were prepared as KBr pellets and the sample concentration was 2 wt.%. The spectra were obtained with 4 cm$^{-1}$ resolution and 64 scans.

1    X-ray diffraction patterns were collected using a PanAnalytical X'Pert Pro diffractometer equipped

2    with multi array X'Celerator detector using Cu Kα radiation generated at 40 kV and 40 mA (λ =

3    1.54056 Å). The diffraction patterns were collected in the 2θ range between 4° and 25° with a step

4    size (Δ2θ) of 0.05° and a counting time of 100 s. Each pattern collection was repeated at least

5    twice on different samples.

6    **Determination of the degree of acetylation (DA)**

7    The degree of acetylation (DA) of the chitin was determined using solid-state nuclear magnetic

8    resonance (NMR). The NMR experiments were performed on a Bruker Advance spectrometer

9    operating at the frequency of 300 MHz for proton (equipped with a 4 mm MAS BB probe) using

10   the combined techniques of crosspolarization (CP) and magic angle spinning (MAS). Field

11   strengths corresponding to 90° pulses of 4.5 μs were used for the matched spinlock cross-

12   polarization transfer $^1$H to $^{13}$C. The contact time was 1 ms, and the recycle delay 10 s. A typical

13   number of 500–3000 scans were acquired for each spectrum. The chemical shifts were externally

14   referred by setting the carbonyl resonance of glycine to 176.03 ppm. Glycine full width at half-

15   height better than 27 Hz. The spinning speed was set at 8000 Hz for all samples. The signals

16   assignment, reported in Figure S1, was done according to literature.[43] The DA was calculated as

17   ratio between the $CH_3$ signal of the acetyl and the average signal of the six carbon of the ring, [43]

18   as follows: $DA = \{I_{CH3} / [(I_{C1} + I_{C2} + I_{C3} + I_{C4} + I_{C5} + I_{C6}) / 6]\} *100$.

19

20   **Results**

21   **β-CnFs preparation and characterization**

Squid pen is composed of proteins, which constitute *ca.* 60 wt.%, and β-chitin, which constitutes about 40 wt%, plus other minor components. β-chitin was isolated from proteins using proteolytic enzymes at acidic and physiological pH, as shown in Figure 1A. The de-proteination process was monitored by measuring the absorption of tryptophan residues at 280 nm (Figure 1B). The spectra showed that this peak disappeared completely following the treatment, which confirmed the complete removal of proteins, at least those containing tryptophan residues.
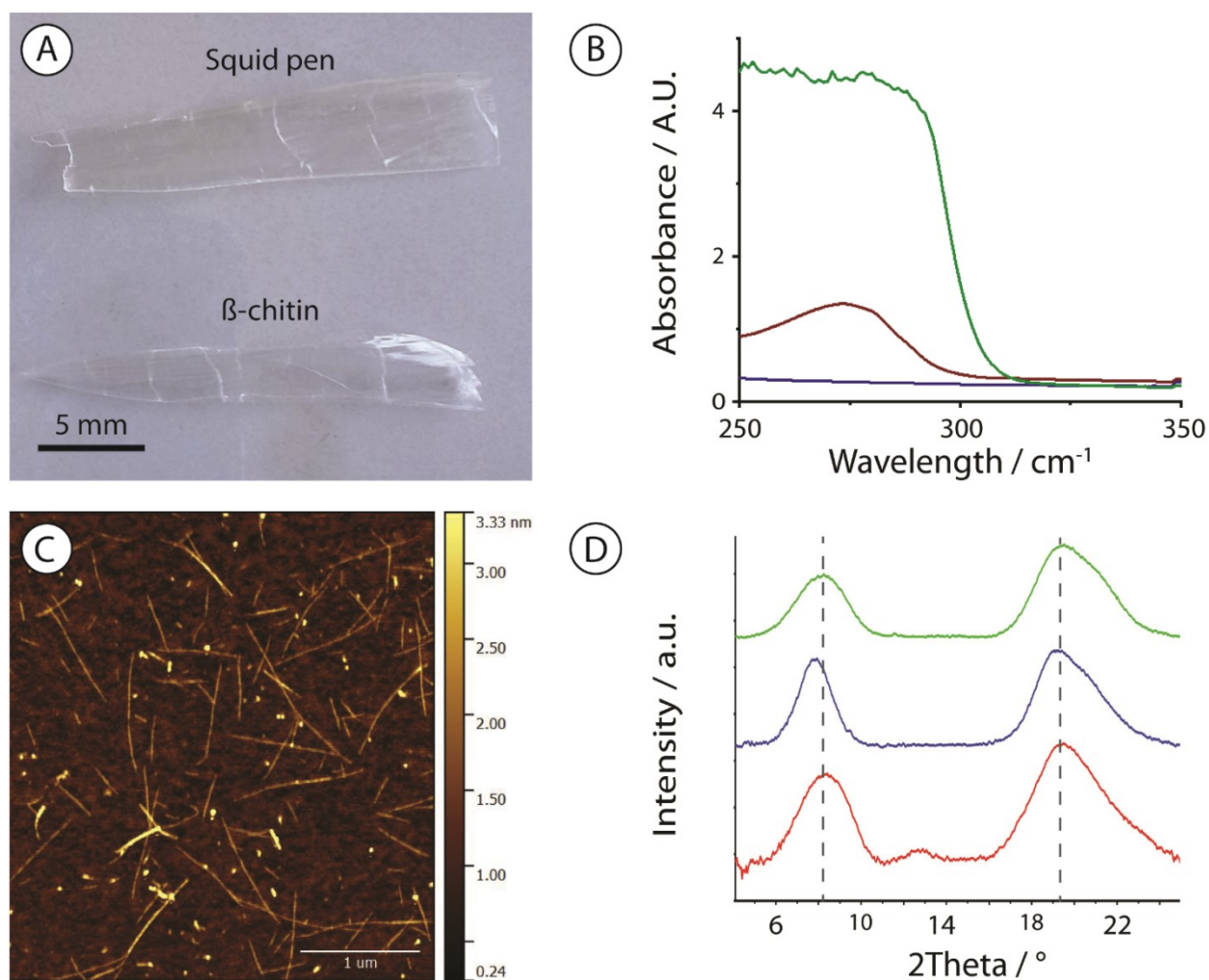


**Figure 1.** (A) A picture of a squid pen and the de-proteinized β-chitin. (B) The UV spectra of a squid pen (green), chitin after the first enzymatic treatment (brown), and purified β-chitin (blue). (C) AFM of the β-CnFs. (D) XRD of a squid pen (green), purified β-chitin (blue), and of a dried β-CnFs dispersion (red). The XRD patterns were shifted on y–axis for the sake of clearness.

1    Optical microscopy confirmed that acidic treatment at pH 3 after the de-proteination process

2    caused the disaggregation of the β-chitin samples in β-CnFs (Figure 2). At a concentration of 0.5

3    mg.mL$^{-1}$ or lower, only few disordered aggregates were present, which were not birefringent when

4    viewed under polarized light. This indicates the absence of crystalline micro-fibers and that the β-

5    CnFs were dispersed by the treatment at low pH. Indeed, AFM analysis on dry samples of β–CnFs

6    at the same concentration revealed the presence of dispersed nanofibrils (Figure 1C). Size

7    measurements revealed two main groups of fibrils with different maximum average lengths, 160

8    ± 50 nm and 340 ± 150 nm respectively, and their height was (2.5 ± 0.3) nm (Figure S1); the latter

9    value may be influenced by the applied load.[44] At a concentration of 1.0 mg mL$^{-1}$, on the other

10   hand, few birefringent microfibers were still present.
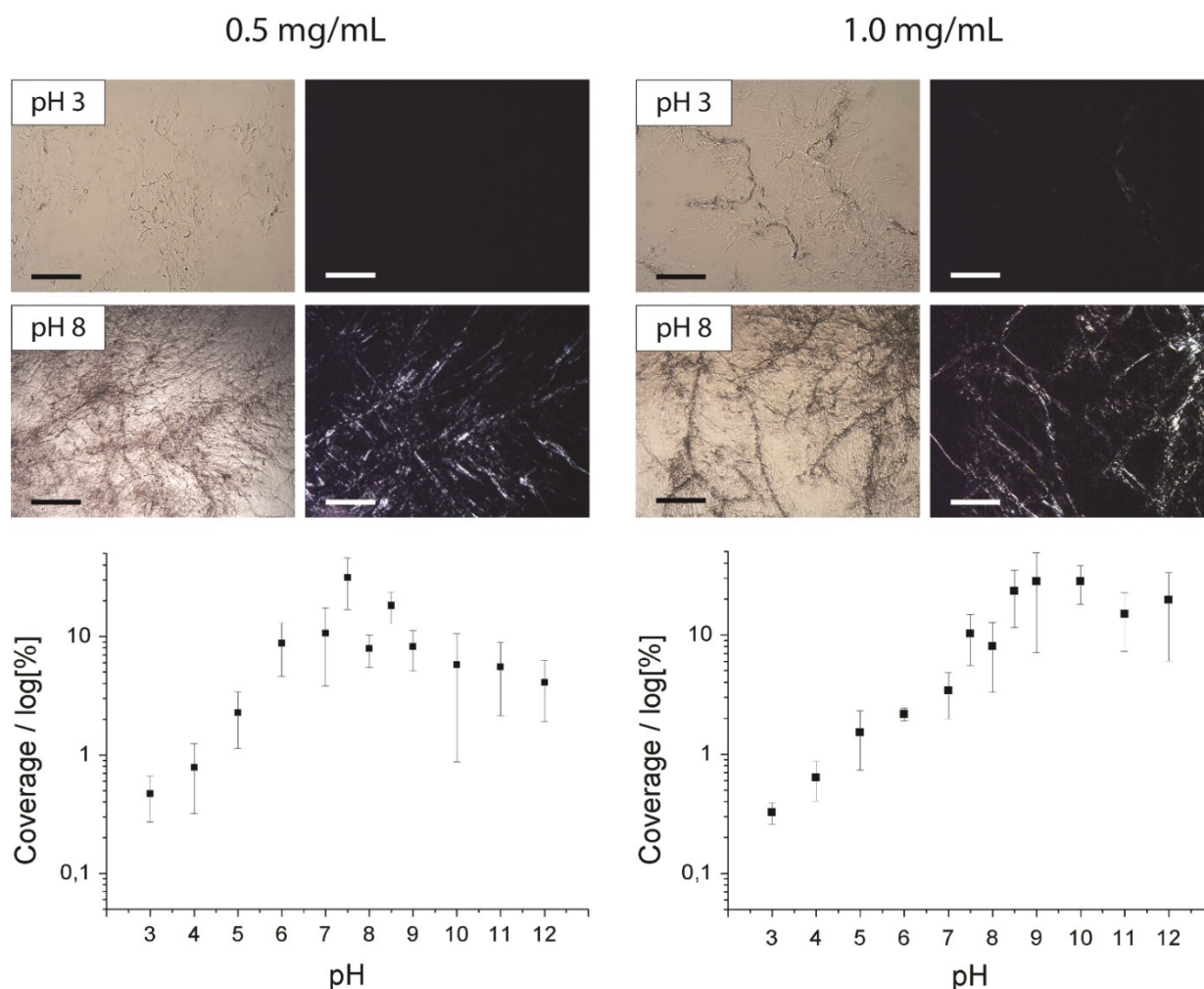
**Figure 2.** Optical microscopy images of β-CnFs self-assembled at different conditions of pH and concentration. On the left, β-CnFs assembled using a 0.5 mg·mL$^{-1}$ dispersion. On the right, β-CnFs assembled using a 1.0 mg·mL$^{-1}$ dispersion. For each concentration an optical image and one with cross-polarizers is reported at pH 3 and 8. Scale bars: 250 μm. Beneath each condition a graph with the fiber coverage at different pHs is shown.

The XRD patterns reported in Figure 1D showed that the squid pen, the chitin isolated using enzymatic digestion, and the β-CnFs dispersion, all conserved the β structure. A shift of the (010) diffraction peak at lower 2θ angle was observed in the purified β-chitin sample. This increment in the unit cell parameter was likely due to the hydration associated to the swelling in the de-proteination treatment.

Solid-state $^{13}C$ NMR demonstrated that the preparation of β-CnFs did not result in the deacetylation of the chitin. The degree of acetylation was above 95 % after the protease treatment, and remained above 93 % in the β-CnFs, after dispersion in acetic acid at pH 3 (Figure S2). It was not possible to determine the degree of acetylation in the squid pen, due to the overlap of chitin and protein signals.
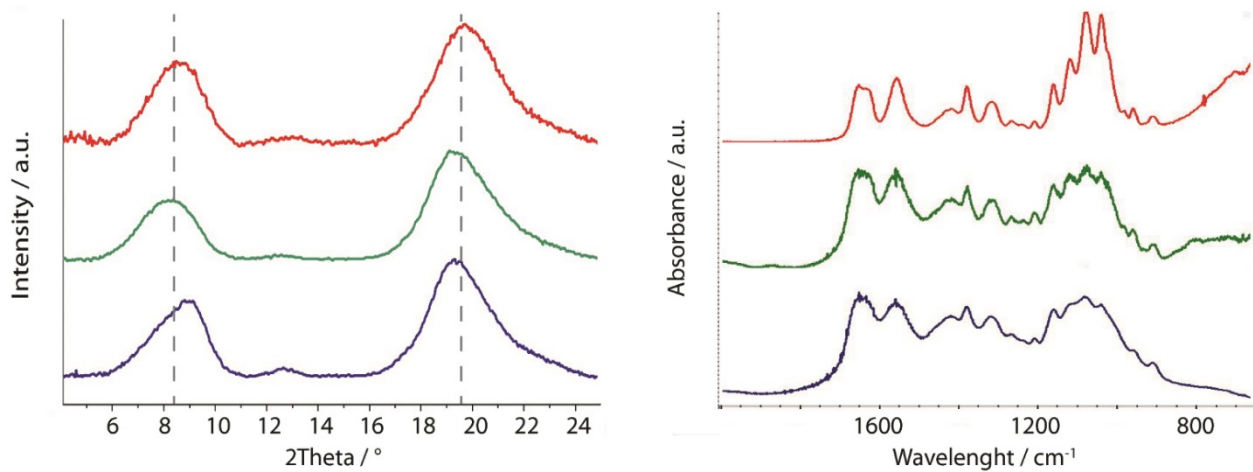
## β-CnFs self-assembly

Since an acidic environment is required for a stable β-CnFs dispersion, we investigated the effect of pH in the self-assembly of the dispersed nanofibrils into microfibrils. This process was followed using bright field and polarized light optical microscopy, whereby the presence of birefringent microfibers was confirmed. Two concentrations of β-CnFs were studied: 0.5 mg·mL$^{-1}$, and 1.0 mg·mL$^{-1}$. The lower concentration resulted in a homogeneous CnFs dispersion, and the higher one gave a mixture of CnFs and micrometric fibers that did not disassemble during the acidic treatment.

We quantified the fibers coverage at each of the pH conditions, as presented in Figure 2. The largest area coverage was observed between pH 7 and 8.5 for the 0.5 mg·mL$^{-1}$ concentration. The higher concentration sample (1 mg·mL$^{-1}$) showed a similar coverage across all the investigated pH conditions above pH 8. At pH 8.5 the two concentrations studied showed a similar fiber coverage (Figure 2 and Figure S3). The average thickness of the fibers at the two concentrations was also similar and not statistically different: $11 \pm 2$ μm for the dispersion at 0.5 mg·mL$^{-1}$, and $13 \pm 3$ μm for the dispersion at 1 mg·mL$^{-1}$ (t-test, p = 0.05, $\nu > 150$). The maximum thickness of the fibers was 18 μm and 15 μm in the β-CnFs 1.0 mg·mL$^{-1}$ and 0.5 mg·mL$^{-1}$ dispersion, respectively. The

1   length was not quantified because the fibers presented a high degree of entanglement and cross-

2   linking, as can be observed in Figure 2.

3   XRD analysis confirmed that chitin was present as the β polymorph in all of the assembled fibers,

4   except that at pH 12. At pH 12 a reduction of the unit cell parameters, which is in agreement with

5   a β- to α-chitin transition, was detected in the X-ray diffraction pattern. As shown in Figure 3, such

6   transition was not visible using FTIR analysis, which showed only the absorption bands originating

7   from the β polymorph (Figure S4).



8

9   **Figure 3.** XRD patterns, on the left, and FTIR spectra, on the right, recorded for β-CnFs assembled
10   at pH 3 (red), 8 (green), and 12 (blue).

11

12   The kinetics of β-CnFs self-assembly at pH 3, 8, and 12 were studied for an aging time from 10

13   min to 72 hours using the 0.5 mg·mL$^{-1}$ β-CnFs dispersion. This particular concentration was

14   selected because it allowed a better evaluation of the self-assembly process due to the absence of

15   starting microfibers. The pH 3 was selected as the most unfavorable condition for self-assembly.

16   The kinetics at pH 8 was investigated since at this pH the higher density of assembled micro-fibers

17   was observed. The experiments at pH 12 were carried out to investigate when the reduction of the

1  unit cell parameters occur. At pH 3 few aggregation processes were observed. After 72 hours, only

2  few non-birefringent fibers that were several micrometers in length were present (Figure S6). In

3  the β-CnFs dispersion at pH 8, on the other hand, birefringent micrometric fibers were observed

4  in less than 10 minutes. Those fibers continued to grow, mostly in length, until growth termination

5  was observed between 24 and 48 hours (Figure S5). At pH 12, first micro-fiber appeared after 10

6  min and the low birefringent micro-fibers growth process was terminated after less than 6 hours.

7  XRD patterns (Figure S6) indicated that the reduction of the unit cell parameters occurred in less

8  than 10 minutes, before the self-assembly process started.

9  Finally, the pH screening revealed a big increment in the microfiber density while transitioning

10  from pH 4 to pH 5. The kinetic study showed that the assembly was less favored at more acidic

11  pH value (see Figure S7 and Figure S8).

12  The optical microscopy data provided information about the assembly of the chitin nanofibers at

13  the micrometer scale. To gain a mechanistic understanding of this process at the nanometer scale,

14  cryo-transmission electron microscopy was used. The study was performed on the 0.5 mg·mL$^{-1}$

15  solution, considering the undesired micro-fibers presence observed in the higher concentration

16  sample (1 mg·mL$^{-1}$). As shown in Figure 4, the assembly occurred in three different steps. Initially,

17  isolated nano-fibrils of 6.4 ± 0.7 nm in diameter and about 100 nm in length were present,

18  apparently not interacting with each another (Figure 4A). 30 seconds after the pH increment the

19  fibrils were observed increasing their length to several hundreds of nanometers, with a diameter

20  of 6.9 ± 0.7 nm (Figure 4B). Those longer fibrils did not show a significant difference in diameter

21  considering the instrument resolution. At 3.5 minutes the fibrils underwent lateral aggregation,

22  forming thicker and loosely organized bundles (Figure 4C, and 4D). Further self-assembly after

1 longer time periods could not be visualized due to the increasing fibers thickness, which eventually

2 prevented electron transmission.
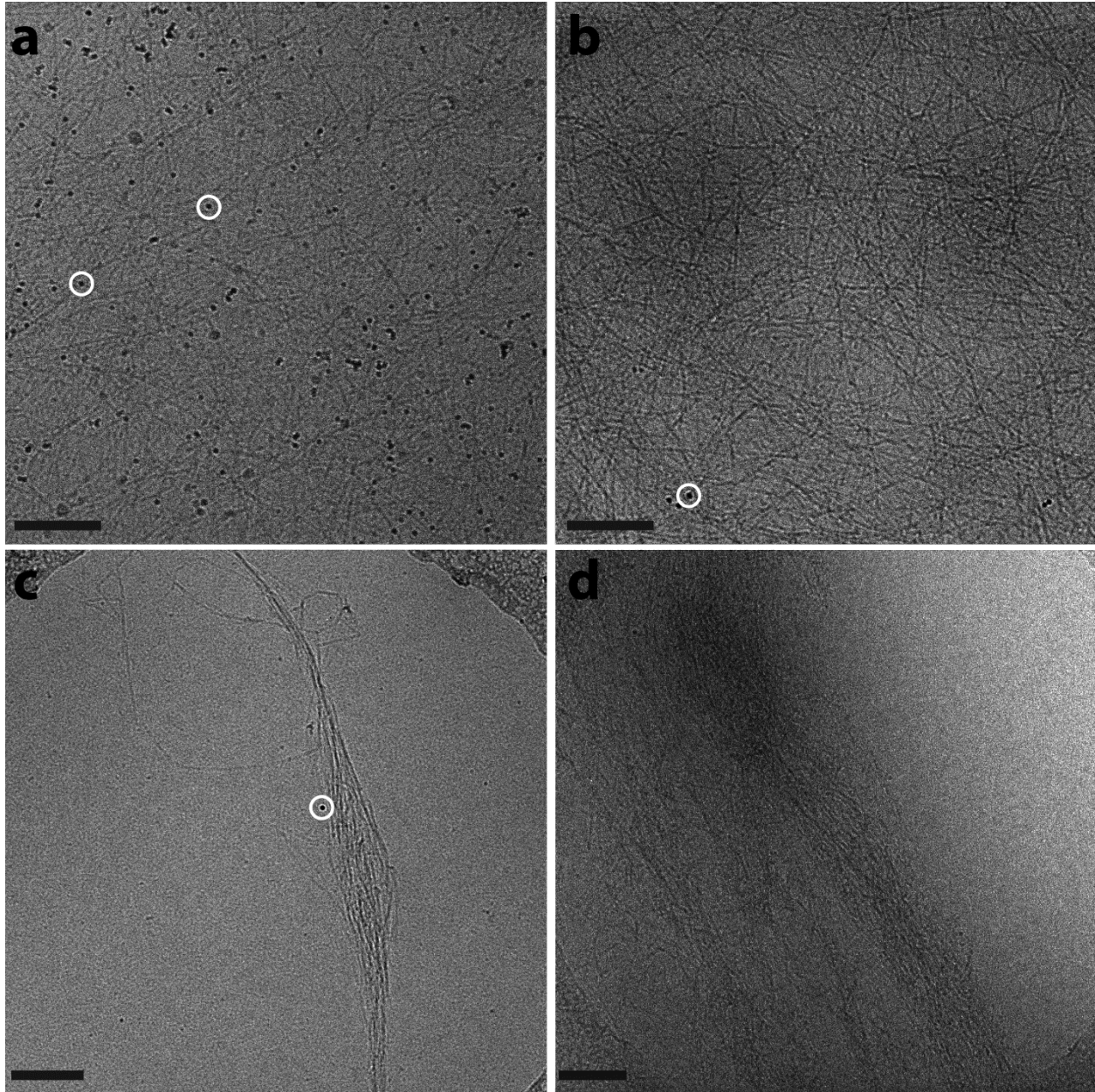


3

4

5 **Figure 4.** Cryo-TEM images of CnFs self-assembled at pH 8. The four different stages of the
6 assembly process are reported: a) at the start of the self-assembly, b-d) different stages observed
7 after 30 seconds. White circles on a-c: 10 nm gold nanoparticles used as fiducial markers. Scale
8 bars: 200 nm.

9

1

## Discussion

### β-CnFs preparation and characterization

4　The aim of this research was to investigate the self-assembly process of β-CnFs in their native

5　aqueous environments. To achieve this goal the first objective was to produce β-CnFs while

6　avoiding the degradation or deacetylation of the N-acetyl D glucosamine residues. For this reason,

7　a mixture of proteolytic enzymes was used, as opposed to the harsh alkaline treatments at high

8　temperatures usually reported in literature.[1]

9　Although proteolytic enzymes promote degradation of squid pen's proteins at physiological pH,

10　usually they do not diffuse into the structure. Because chitin swells at acidic pH values[45,46], pepsin

11　– optimally active at acidic pH – was used. Under these conditions the enzyme diffused into the

12　squid pen and catalyzed the degradation of the proteins in the whole material. Such a swelling,

13　crucial for the enzyme diffusion, was preserved by keeping the pen hydrated during the trypsin

14　enzymatic peptides hydrolysis at physiological pH. Subsequently, β-CnFs were obtained in a mild

15　acidic environment exploiting the friction forces induced by the mechanical mixing. In this way

16　the β-chitin films disassembled to β-CnFs. The fibrils obtained showed a diameter of $6.4 \pm 0.7$ nm,

17　when observed in the hydrate state using cryo-TEM, and one of $2.5 \pm 0.3$ nm, when observed dry

18　using AFM. It is possible that the dehydration of the nanofibers for AFM measurements resulted

19　in the shrinkage of the structure, hence the difference in the diameter obtained from the two

20　techniques. Alternatively, it is also possible that the load applied during the AFM measurement

21　resulted in the compression of the nanofibril and hence a smaller diameter.

It is important to note that the disaggregation of the squid pen into β-CnFs under acidic conditions was only possible after proteinase treatment. Similarly, digestion of the chitin using chitinase was only possible after the squid pen was deproteinated. These results suggest that proteins in the squid pen may have a protective role against chitin disassembly, and biodegradation in physiological condition.

It natural matrices chitin is not completely acetylated[47,48] and the amino groups of the deacetylated chitin units are hypothesized to covalently bind proteins. The chitin obtained from the proteolytic enzyme digestion had a DA above 95%. The free amino groups were protonated during the acidic disassembly of chitin favoring its disaggregation by electrostatic repulsions. Chitin with lower DA, obtained from alkaline treatments, was observed to disaggregate in the same experimental conditions as used here. Interesting, no disaggregation was reported for DA below 83% and above 55%.[49] Considering the high DA and the insolubility of more deacetylated chitins, we estimate that the disaggregation observed was due partially to charge repulsion between the amino groups and mostly to a swelling of the regions between the crystal domains due to the squid pen structural organization, visible by the swelling of the material. As a result, mechanical stirring forces cause the dispersion of nanofibrils. This observation would explain why nano-fibrils and not single molecules were obtained, why the disassembly kinetic was slow, and why the disassembly worked only under strong the mechanical action of the stirring bar (only a strong swelling was observed without stirring). Overall, all the above observations indicate that the $\leq 7\%$ of positive charge present in the CnFs at pH 3 contributed to the stabilization of the nanofibril dispersion.

**β-CnFs self-assembly**

1    The choice of β-CnFs as starting material to investigate the self-assembly has been guided by two

2    main reasons: (i) when single polymeric chains are used they always assemble in α-chitin;[50] (ii) in

3    biological systems the interaction of chitin with other molecules, as proteins, occurs when chitin

4    is already assembled in nano-fibrils.[9,51,52,53]

5    The β-CnFs self-assembly was induced by increasing the pH. The pH controlled self-assembly of

6    materials in biological systems has been already observed in other bio-macromolecules,[54,55,56] and

7    is relevant in the biomineralization of biominerals.[57,58] In this context the identification of the pH

8    value at which the self-assembly occurs can provide information on the features of the biological

9    site where the assembly takes place.

10   The results of the present study of β-CnFs self-assembly provided at least four novel pieces of

11   information. First, pH 7-8.5 is the optimal range for the formation of the micro-fibers starting from

12   the 0.5 mg·mL$^{-1}$ β-CnFs homogeneous dispersion. Interestingly, this pH range includes

13   physiological pHs,[59,60] and that of seawater, which ranges between 8.0 and 8.2.[56,61] This result

14   shows how chitin assembly can occur compatibly inside the living organism, as in cephalopods

15   internal skeletal matrices,[9,62] or as an external process. This last possibility includes processes

16   where the pH is that of sea water, as in marine calcifying organisms,[63,64] and processes where the

17   pH is defined by the fluids secreted by the animal, as for terrestrial insects' exoskeletons.

18   Moreover, these pH values are relevant in the precipitation process of calcium carbonate, a mineral

19   that is commonly associated to chitin in calcified tissues.[65,66] In the pH range 7-8.5 the deposition

20   of calcium carbonate almost does not occur, while it takes place at pH ≥ 8.5. This indicates that

21   the assembly of β-CnFs to form β-chitin fibers occurs before the precipitation of calcium carbonate

22   takes place. This hypothesis is in agreement with the current model of preformed organic matrix

23   guiding the textural organization of calcium carbonate crystals.[67]

1   A second finding is the polymorphic stability of the β-CnFs even at pH 12, as deductible from the

2   combination of the FTIR and X-ray diffraction data. They show that only a unit cell parameter

3   contraction occurs (from $10.24 \pm 0.06$ Å to $9.8 \pm 0.1$ Å for the (010) peak). It is reported that the

4   β- to α-chitin transition occurs at room temperature in very alkaline ($[OH^-] > 10$ mol·L$^{-1}$)[68] or

5   acidic ($[H_3O^+] > 7$ mol·L$^{-1}$)[45,46] solutions, or in non-aqueous solvents[50] and that this process always

6   occurred after a disassembly to single molecules and a successive reassembly.[49] It could be

7   speculated that the contraction of the unit cell might be an initial step for a structural β- to α-chitin

8   re-organization that does not affect the polymorphism of the β-CnFs.

9   The third point is related to the extent of the self-assembly as a function of the β-CnFs

10  concentration. Despite the fiber's thickness, evaluated at pH 8.5, was not significantly different

11  for the two concentrations, the maximum fiber's thickness in the 1.0 mg·mL$^{-1}$ concentration is

12  higher than the 0.5 mg·mL$^{-1}$ one (about 18 μm and 15 μm respectively). Qualitatively the 1.0

13  mg·mL$^{-1}$ concentration showed also longer fibers compared to the 0.5 mg·mL$^{-1}$ one. These

14  observations do not fit just with the doubling of the concentration. It has to be considered that in

15  the 1.0 mg·mL$^{-1}$ β-CnFs heterogeneous dispersion some micro-fibers were still present from the

16  disassembly process. These fibers could act as template for the β-CnFs assembling. This possibility

17  is intriguing because in living organisms chitin deposition can occur also on previously assembled

18  fibers. Moreover, despite showing shorter and thinner final β-chitin fibers, the lower concentration

19  exhibited a comparable coverage in the image analysis, meaning that more fibers nucleated in the

20  process. This result, combined with the two different pH range of preferred self-assembly, may

21  indicate the fibers' preference to nucleate in the pH range between 7 and 8.5 and to grow at pH

22  over 8.5.

The last finding comes from the analyses of the cryo-TEM observations. The β-CnFs were observed to assemble in three distinct steps: i) increase their length, ii) assemble in 1D organized bundle, and iii) assemble in bundles of bundles until getting their final dimension. It was not possible to detect a relevant increment in the fibrils thickness in the first step. However, during their growth the β-CnFs started aggregating laterally as well, forming loosely packed bundles. In nature chitin fibrils are frequently wrapped in a protein folder, as in insect cuticle,[44][45] nacre organic matrix,[51] or in the squid pen.[9] Our observations indicate that these proteins play a crucial role in the perfectly registered chitin self-assembly. Alternatively, the disordered assembly could have resulted from the rapid change of the environment. Since the presence of buffer molecules can affect β-CnFs nucleation and aggregation, the chemical system was kept as simple as possible, controlling the pH only by adding an acid or a base.

It could be argued that the self-assembly of the nanofibers was caused by the deprotonation of the primary amines in the deacetylated monomers once the pH was raised above the p$K_a$ of the amino groups (about 6.3[69,70,71,72]), effectively eliminating the electrostatic repulsion between nanofibrils. Here, we note that the DA of the β-CnF dispersion was at ≥ 93%. We hypothesize that these charged units play an important role in the stability of the nano-fibrils in water and that their deprotonation was the first trigger for chitin assembly.. Considering, however, that only ≤ 7 % of the monomeric units were deacetylated, it is likely that deprotonation is not enough to drive the self-assembly, and that other forms of intermolecular interactions are also involved. Indeed, if the self-assembly was only caused by the deprotonation of the amino groups, one would expect the aggregation of the nanofibrils to occur at pHs closed to 6.3, where already less than 3.5% (50% of the amino groups) of the chitin units are charged, rather than 8. The slight decrease in the coverage for the 0.5 mg·mL$^{-1}$ dispersion at pH over 8.5 also would not be expected.

These results show a propensity for the β-CnFs to aggregate in large 1D organized structures (micrometric in diameter and millimetric in length) despite their non-specific interactions. We speculate that in living organisms proteins provide a greater control over the chitin fibrils self-assembly process (especially in lateral packing), and direct their growth towards organized macro-structures.

**Conclusion**

The aim of this research was to study the self-assembly of β-CnFs into β-chitin fibers in aqueous environments. Our first objective was to design an experimental system where chitin would exhibit features as close to the natural material as possible, and would be able to self-assemble. This goal was achieved by preparing stable dispersions in acidic conditions of β-CnFs from the squid pen β-chitin. Self-assembly process was triggered by increasing the pH of those dispersions to mild basic values whereby the kinetics of that process was regulated by the adjustment of the starting pH.

The main discoveries, on β-CnFs self assembly to fibers, utilizing this system have been: 1) the nucleation is favored around pH 8, which is very close to both physiological, and seawater pHs; 2) they maintain the β-polymorph for the whole process, showing a shrinkage of the unit cell parameter at basic pH; 3) the self-assembly is favored on previously grown fibers; 4) they grow preferentially at pH above 8.5 up to a maximum value in thickness.

The β-CnFs self-assembly observation by cryo-TEM showed a three-step process. Firstly the β-CnFs self-assembled and increased their length, and then formed bundles that finally aggregated into fibers until they reached macroscopic dimensions. Beside these important and novel information, the β-CnFs water dispersions represent an adaptable and flexible platform to study

chitin self-assembly and chitin interaction with structural chitin-binding proteins, as much as any

other chitin-interacting molecule.

## ASSOCIATED CONTENT

Missing data reported in the text, such as chitin assembly along the time or the complete

assembly screening, can be found in the Supporting Information.

## AUTHOR INFORMATION

**Corresponding Author**

Prof. Giuseppe Falini (giuseppe.falini@unibo.it) and Prof. Fabio Nudelman
(fabio.nudelman@ed.ac.uk).

**Present Addresses**

† UK Research and Innovation, Research Complex at Harwell, Rutherford Appleton Laboratory,

Harwell, OX11 0FA, UK

**Author Contributions**

DM, BM, and FV performed the experiments; GF conceived the study; DM, GF, and FN designed

the experiments; The manuscript was written through contributions of all authors. All authors have

given approval to the final version of the manuscript.

6 ABBREVIATIONS

7 CnF, Chitin nano-fibrils; FTIR, Fourier-transform infrared spectroscopy; XRD, X-ray Powder

8 Diffraction; SEM, Scanning Elecron Microscopy; TEM, Transmission electron microscopy.

9

REFERENCES

(1)    Ianiro, A.; Giosia, M.; Fermani, S.; Samorì, C.; Barbalinardo, M.; Valle, F.; Pellegrini, G.; Biscarini, F.; Zerbetto, F.; Calvaresi, M.; Falini G. Customizing Properties of β-Chitin in Squid Pen (Gladius) by Chemical Treatments. *Mar. Drugs* **2014**, *12* (12), 5979–5992. https://doi.org/10.3390/md12125979.

(2)    Youn, D. K.; No, H. K.; Prinyawiwatkul, W. Preparation and Characteristics of Squid Pen β-Chitin Prepared under Optimal Deproteinisation and Demineralisation Condition. *Int. J. Food Sci. Technol.* **2013**, *48*, 571–577. https://doi.org/10.1111/ijfs.12001.

(3)    Brine, C. J.; Austin, P. R. Chitin Isolates: Species Variation in Residual Amino Acids. *Comp. Biochem. Physiol.* **1981**, *70B*, 173–178. https://doi.org/10.1016/0305-0491(81)90031-6.

(4)    Blackwell, J.; Gardner, K. H.; Kolpak, F. J.; Minke, R.; Classey, W. B. Refinement of Cellulose and Chitin Structures. *ACS Symp. Ser.* **1980**, *141*, 315–334.

(5)    Jang, M. K.; Kong, B. G.; Jeong, Y. Il; Lee, C. H.; Nah, J. W. Physicochemical Characterization of α-Chitin, β-Chitin, and γ-Chitin Separated from Natural Resources. *J. Polym. Sci. Part A Polym. Chem.* **2004**, *42*, 3423–3432. https://doi.org/10.1002/pola.20176.

(6)    Cohn, W. E. *Advances in Insect Physiology*; Elsevier: London and New York, 1963.

(7)    Lin, Q.; Gourdon, D.; Sun, C.; Holten-Andersen, N.; Anderson, T. H.; Waite, J. H.; Israelachvili, J. N. Adhesion Mechanisms of the Mussel Foot Proteins Mfp-1 and Mfp-3. *Proc. Natl. Acad. Sci. U. S. A.* **2007**, *104* (10), 3782–3786. https://doi.org/10.1073/pnas.0607852104.

(8)    Kurita, K.; Ishii, S.; Tomita, K.; Nishimura, S.-I.; Shimoda, K. Reactivity Characteristics of Squid β-Chitin as Compared with Those of Shrimp Chitin: High Potentials of Squid Chitin

as a Starting Material for Facile Chemical Modifications. *J. Polym. Sciece* **1944**, *32*, 1027–1032.

(9)  Yang, F. C.; Peters, R. D.; Dies, H.; Rheinstädter, M. C. Hierarchical, Self-Similar Structure in Native Squid Pen. *Soft Matter* **2014**, *10*, 5541–5549. https://doi.org/10.1039/c4sm00301b.

(10)  Weiss, I. M.; Schönitzer, V. The Distribution of Chitin in Larval Shells of the Bivalve Mollusk Mytilus Galloprovincialis. *J. Struct. Biol.* **2006**, *153*, 264–277. https://doi.org/10.1016/j.jsb.2005.11.006.

(11)  Mackinder, L.; Wheeler, G.; Schroeder, D.; Riebesell, U.; Brownlee, C. Molecular Mechanisms Underlying Calcification in Coccolithophores. *Geomicrobiol. J.* **2010**, *27*, 585–595. https://doi.org/10.1080/01490451003703014.

(12)  Nudelman, F.; Shimoni, E.; Klein, E.; Rousseau, M.; Bourrat, X.; Lopez, E.; Addadi, L.; Weiner, S. Forming Nacreous Layer of the Shells of the Bivalves Atrina Rigida and Pinctada Margaritifera: An Environmental- and Cryo-Scanning Electron Microscopy Study. *J. Struct. Biol.* **2008**, *162*, 290–300. https://doi.org/10.1016/j.jsb.2008.01.008.

(13)  Kaya, M.; Mujtaba, M.; Ehrlich, H.; Salaberria, A. M.; Baran, T.; Amemiya, C. T.; Galli, R.; Akyuz, L.; Sargin, I.; Labidi, J. On Chemistry of γ-Chitin. *Carbohydr. Polym.* **2017**, *176*, 177–186. https://doi.org/10.1016/j.carbpol.2017.08.076.

(14)  Heim, M.; Römer, L.; Scheibel, T. Hierarchical Structures Made of Proteins. the Complex Architecture of Spider Webs and Their Constituent Silk Proteins. *Chem. Soc. Rev.* **2010**, *39*, 156–164. https://doi.org/10.1039/b813273a.

(15)  Komai, Y.; Ushiki, T. The Three-Dimensional Organization of Collagen Fibrils in the Human Cornea and Sclera. *Investig. Ophthalmol. Vis. Sci.* **1991**, *32* (8), 2244–2258.

1          https://doi.org/http://dx.doi.org/10.1016/j.nimb.2015.12.002.

(16)    Autumn, K. Gecko Adhesion: Structure, Function, and Applications. *MRS Bull.* **2007**, *32*, 473–478. https://doi.org/10.1097/HPC.0b013e3181a84613.

(17)    Montroni, D.; Valle, F.; Rapino, S.; Fermani, S.; Calvaresi, M.; Harrington, M. J.; Falini, G. Functional Biocompatible Matrices from Mussel Byssus Waste. *ACS Biomater. Sci. Eng.* **2018**, *4*, 57–65. https://doi.org/10.1021/acsbiomaterials.7b00743.

(18)    Raabe, D.; Romano, P.; Sachs, C.; Fabritius, H.; Al-Sawalmih, A.; Yi, S. B.; Servos, G.; Hartwig, H. G. Microstructure and Crystallographic Texture of the Chitin-Protein Network in the Biological Composite Material of the Exoskeleton of the Lobster Homarus Americanus. *Mater. Sci. Eng. A* **2006**, *421*, 143–153. https://doi.org/10.1016/j.msea.2005.09.115.

(19)    Huang, J.; Zhong, Y.; Zhang, L.; Cai, J. Extremely Strong and Transparent Chitin Films: A High-Efficiency, Energy-Saving, and "Green" Route Using an Aqueous KOH/Urea Solution. *Adv. Funct. Mater.* **2017**, *27*, 1701100. https://doi.org/10.1002/adfm.201701100.

(20)    Weaver, J. C.; Milliron, G. W.; Miserez, A.; Evans-lutterodt, K.; Herrera, S.; Gallana, I.; Mershon, W. J.; Swanson, B.; Zavattieri, P.; Dimasi, E.; Kisalius, D. The Stomatopod Dactyl Club : A Formidable Damage-Tolerant Biological Hammer. *Science* **2012**, *336*, 1275–1280. https://doi.org/10.1126/science.1218764.

(21)    Politi, Y.; Priewasser, M.; Pippel, E.; Zaslansky, P.; Hartmann, J.; Siegel, S.; Li, C.; Barth, F. G.; Fratzl, P. A Spider's Fang: How to Design an Injection Needle Using Chitin-Based Composite Material. *Adv. Funct. Mater.* **2012**, *22*, 2519–2528. https://doi.org/10.1002/adfm.201200063.

(22)    Finlayson, E. D.; McDonald, L. T.; Vukusic, P. Optically Ambidextrous Circularly

Polarized Reflection from the Chiral Cuticle of the Scarab Beetle Chrysina Resplendens. *J. R. Soc. Interface* **2017**, *14*. https://doi.org/10.1098/rsif.2017.0129.

(23)  Gaill, F.; Persson, J.; Sugiyama, J.; Vuong, R.; Chanzy, H. The Chitin System in the Tubes of Deep Sea Hydrothermal Vent Worms. *J. Struct. Biol.* **1992**, *109*, 116–128. https://doi.org/10.1016/1047-8477(92)90043-A.

(24)  Wysokowski, M.; Petrenko, I.; Stelling, A. L.; Stawski, D.; Jesionowski, T.; Ehrlich, H. Poriferan Chitin as a Versatile Template for Extreme Biomimetics. *Polymers (Basel).* **2015**, *7*, 235–265. https://doi.org/10.3390/polym7020235.

(25)  Wu, J.; Meredith, J. C. Assembly of Chitin Nanofibers into Porous Biomimetic Structures via Freeze Drying. *ACS Macro Lett.* **2014**, *3*, 185–190. https://doi.org/10.1021/mz400543f.

(26)  Zhong, C.; Cooper, A.; Kapetanovic, A.; Fang, Z.; Zhang, M.; Rolandi, M. A Facile Bottom-up Route to Self-Assembled Biogenic Chitin Nanofibers. *Soft Matter* **2010**, *6*, 5298–5301. https://doi.org/10.1002/anie.201703784.

(27)  Jin, J.; Hassanzadeh, P.; Perotto, G.; Sun, W.; Brenckle, M. A.; Kaplan, D.; Omenetto, F. G.; Rolandi, M. A Biomimetic Composite from Solution Self-Assembly of Chitin Nanofibers in a Silk Fibroin Matrix. *Adv. Mater.* **2013**, *25*, 4482–4487. https://doi.org/10.1002/adma.201301429.

(28)  Fox, J. D.; Capadona, R.; Marasco, P. D.; Rowan, S. J. Bioinspired Water-Enhanced Mechanical Gradient Nanocomposite Films That Mimic the Architecture and Properties of the Squid Beak. *J. Am. Chem. Soc.* **2013**, *135*, 5167–5174. https://doi.org/10.1021/ja4002713.

(29)  Falini, G.; Fermani, S.; Ripamonti, A. Crystallization of Calcium Carbonate Salts into Beta-Chitin Scaffold. *J. Inorg. Biochem.* **2002**, *91*, 475–480.

(30) Deparis, O.; Vandenbem, C.; Rassart, M.; Welch, V. L.; Vigneron, J. Color-Selecting Reflectors Inspired from Biological Periodic Multilayer Structures. *Opt. Express* **2006**, *14* (8), 3547–3555.

(31) Mulisch, M. Chitin in Protistan Organisms: Distribution, Synthesis and Deposition. *Eur. J. Protistol.* **1993**, *29*, 1–18. https://doi.org/10.1016/S0932-4739(11)80291-9.

(32) Bartnicki-Garcia, S.; Skjak-Brsek, G.; Anthonsen, T.; Sandford, P. Chitin and Chitosan. Sources, Chemistry, Biochemistry, Physical Properties and Applications. In *The biochemical cytology of chitin and chitosan synthesis in fungi*; London and New York, 1989; pp 23–35.

(33) Gupta, N. S. *Chitin Formation and Diagenesis*; Editor, S., Ed.

(34) Merzendorfer, H. Insect Chitin Synthases: A Review. *J. Comp. Physiol. B* **2006**, *176*, 1–15. https://doi.org/10.1007/s00360-005-0005-3.

(35) Weiss, I. M.; Schönitzer, V.; Eichner, N.; Sumper, M. The Chitin Synthase Involved in Marine Bivalve Mollusk Shell Formation Contains a Myosin Domain. *FEBS Lett.* **2006**, *580*, 1846–1852. https://doi.org/10.1016/j.febslet.2006.02.044.

(36) Weiss, I. M.; Lüke, F.; Eichner, N.; Guth, C.; Clausen-Schaumann, H. On the Function of Chitin Synthase Extracellular Domains in Biomineralization. *J. Struct. Biol.* **2013**, *183*, 216–225. https://doi.org/10.1016/j.jsb.2013.04.011.

(37) Falini, G.; Reggi, M.; Fermani, S.; Sparla, F.; Goffredo, S.; Dubinsky, Z.; Levi, O.; Dauphin, Y.; Cuif, J. P. Control of Aragonite Deposition in Colonial Corals by Intra-Skeletal Macromolecules. *J. Struct. Biol.* **2013**, *183*, 226–238. https://doi.org/10.1016/j.jsb.2013.05.001.

(38) Goffredo, S.; Vergni, P.; Reggi, M.; Caroselli, E.; Sparla, F.; Levy, O.; Dubinsky, Z.; Falini,

G. The Skeletal Organic Matrix from Mediterranean Coral Balanophyllia Europaea Influences Calcium Carbonate Precipitation. *PLoS One* **2011**, *6* (7), 1–12. https://doi.org/10.1371/journal.pone.0022338.

(39) Dunn, B. M. Structure and Mechanism of the Pepsin-like Family of Aspartic Peptidases. *Chem. Rev.* **2002**, *102* (12), 4431–4458. https://doi.org/10.1021/cr010167q.

(40) Radisky, E. S.; Lee, J. M.; Lu, C.-J. K.; Koshland, D. E. Insights into the Serine Protease Mechanism from Atomic Resolution Structures of Trypsin Reaction Intermediates. *PNAS* **2006**, *103* (18), 6835–6840. https://doi.org/10.1073/pnas.0601910103.

(41) Fan, Y.; Saito, T.; Isogai, A. Preparation of Chitin Nanofibers from Squid Pen β-Chitin by Simple Mechanical Treatment under Acid Conditions. *Biomacromolecules* **2008**, *9*, 1919–1923. https://doi.org/10.1021/bm800178b.

(42) Antosova, A.; Gazova, Z.; Fedunova, D.; Valusova, E.; Bystrenova, E.; Valle, F.; Daxnerova, Z.; Biscarini, F.; Antalik, M. Anti-Amyloidogenic Activity of Glutathione-Covered Gold Nanoparticles. *Mater. Sci. Eng. C* **2012**, *32*, 2529–2535. https://doi.org/10.1016/j.msec.2012.07.036.

(43) Heux, L.; Brugnerotto, J.; Desbriéres, J.; Versali, M. F.; Rinaudo, M. Solid State NMR for Determination of Degree of Acetylation of Chitin and Chitosan. *Biomacromolecules* **2000**, *1*, 746–751. https://doi.org/10.1021/bm000070y.

(44) Iannazzo, D.; Mazzaglia, A.; Scala, A.; Pistone, A.; Galvagno, S.; Lanza, M.; Riccucci, C.; Ingo, G. M.; Colao, I.; Sciortino, M. T.; Valle, F. β-Cyclodextrin-Grafted on Multiwalled Carbon Nanotubes as Versatile Nanoplatform for Entrapment of Guanine-Based Drugs. *Colloids Surfaces B Biointerfaces* **2014**, *123*, 264–270. https://doi.org/10.1016/j.colsurfb.2014.09.025.

1   (45)   Saito, Y.; Okano, T.; Gaill, F.; Chanzy, H.; Putaux, J.-L. Structural Data on the Intra-

2         Crystalline Swelling of β-Chitin. *Int. J. Biol. Macromol.* **2000**, *28*, 81–88.

3         https://doi.org/10.1016/S0141-8130(00)00147-1.

4   (46)   Saito, Y.; Putaux, J. L.; Okano, T.; Gaill, F.; Chanzy, H. Structural Aspects of the Swelling

5         of β Chitin in HCl and Its Conversion into α Chitin. *Macromolecules* **1997**, *30* (13), 3867–

6         3873. https://doi.org/10.1021/ma961787+.

7   (47)   Hackman, R. H. Studies on Chitin IV. The Occurrence of Complexes in Which Chitin and

8         Protein Are Covalently Linked. *Aust. J. Biol. Sci.* **1960**, *13* (4), 568–577.

9   (48)   Gottschalk, A.; Murphy, W. H.; Graham, E. R. B. Carbohydrate-Peptide Linkages in

10        Glycoproteins and Methods for Their Elucidation. *Nature* **1962**, *194*, 1051–1053.

11   (49)   Montroni, D.; Fermani, S.; Morellato, K.; Torri, G.; Naggi, A.; Cristofolini, L.; Falini, G.

12        β-Chitin Samples with Similar Microfibril Arrangement Change Mechanical Properties

13        Varying the Degree of Acetylation. *Carbohydr. Polym.* **2019**, *207*, 26–33.

14        https://doi.org/10.1016/j.carbpol.2018.11.069.

15   (50)   Rolandi, M.; Rolandi, R. Self-Assembled Chitin Nano Fibers and Applications. *Adv.*

16        *Colloid Interface Sci.* **2014**, *207*, 216–222.

17   (51)   Weiss, I. M.; Renner, C.; Strigl, M. G.; Fritz, M. A Simple and Reliable Method for the

18        Determination and Localization of Chitin in Abalone Nacre. *Chem. Mater.* **2002**, *14*, 3252–

19        3259. https://doi.org/10.1021/cm001217v.

20   (52)   Blackwell, J.; Weih, M. A. Structure of Chitin-Protein Complexes: Ovipositor of the

21        Ichneumon Fly Megarhyssa. *J. Mol. Biol.* **1980**, *137*, 49–60. https://doi.org/10.1016/0022-

22        2836(80)90156-4.

23   (53)   Neville, A. C.; Luke, B. M. A Two-System Model for Chitin-Protein Complexes in Insect

1    Cuticles. *Tissue Cell* **1969**, *1* (4), 689–707.

2    (54)  Cui, F. Z.; Li, Y.; Ge, J. Self-Assembly of Mineralized Collagen Composites. *Mater. Sci.*

3          *Eng. R Reports* **2007**, *57*, 1–27. https://doi.org/10.1016/j.mser.2007.04.001.

4    (55)  Askarieh, G.; Hedhammar, M.; Nordling, K.; Saenz, A.; Casals, C.; Rising, A.; Johansson,

5          J.; Knight, S. D. Self-Assembly of Spider Silk Proteins Is Controlled by a PH-Sensitive

6          Relay. *Nature* **2010**, *465*, 236–238. https://doi.org/10.1038/nature08962.

7    (56)  Priemel, T.; Degtyar, E.; Dean, M. N.; Harrington, M. J. Rapid Self-Assembly of Complex

8          Biomolecular Architectures during Mussel Byssus Biofabrication. *Nat. Commun.* **2017**, *8*,

9          14539. https://doi.org/10.1038/ncomms14539.

10   (57)  Hammes, F.; Verstraete, W. Key Roles of PH and Calcium Metabolism in Microbial

11         Carbonate Precipitation. *Rev. Environ. Sci. Biotechnol.* **2002**, *1* (1), 3–7.

12         https://doi.org/10.1023/A:1015135629155.

13   (58)  Bradt, J.-H.; Mertig, M.; Teresiak, A.; Pompe, W. Biomimetic Mineralization of Collagen

14         by Combined Fibril Assembly and Calcium Phosphate Formation. *Chem. Mater.* **1999**, *11*,

15         2694–2701. https://doi.org/10.1021/cm991002p.

16   (59)  Boron, W. F.; De Weer, P. Intracellular PH Transients in Squid Giant Axons Caused by

17         $CO_2$, $NH_3$, and Metabolic Inhibitors. *J. Gen. Physiol.* **1976**, *67*, 91–112.

18         https://doi.org/10.1085/jgp.67.1.91.

19   (60)  Casey, J. R.; Grinstein, S.; Orlowski, J. Sensors and Regulators of Intracellular PH. *Nat.*

20         *Rev. Mol. Cell Biol.* **2010**, *11*, 50–61. https://doi.org/10.1038/nrm2820.

21   (61)  Clark, D.; Lamare, M.; Barker, M. Response of Sea Urchin Pluteus Larvae (Echinodermata:

22         Echinoidea) to Reduced Seawater PH: A Comparison among a Tropical, Temperate, and a

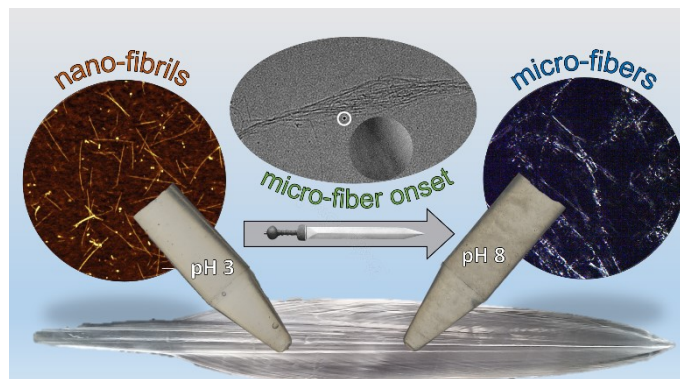23         Polar Species. *Mar. Biol.* **2009**, *156*, 1125–1137. https://doi.org/10.1007/s00227-009-1155-

8.

(62)    Florek, M.; Fornal, E.; Gómez-Romero, P.; Zieba, E.; Paszkowicz, W.; Lekki, J.; Nowak, J.; Kuczumow, A. Complementary Microstructural and Chemical Analyses of Sepia Officinalis Endoskeleton. *Mater. Sci. Eng. C* **2009**, *29*, 1220–1226. https://doi.org/10.1016/j.msec.2008.09.040.

(63)    Kröger, N. The Molecular Basis of Nacre Formation. *Science (80-. ).* **2009**, *325*, 1351–1352. https://doi.org/10.1126/science.1177055.

(64)    Fu, G.; Valiyaveettil, S.; Wopenka, B.; Morse, D. E. CaCO3 Biomineralization: Acidic 8-KDa Proteins Isolated from Aragonitic Abalone Shell Nacre Can Specifically Modify Calcite Crystal Morphology. *Biomacromolecules* **2005**, *6*, 1289–1298. https://doi.org/10.1021/bm049314v.

(65)    Mikkelsen, A.; Engelsen, S. B.; Hansen, H. C. B.; Larsen, O.; Skibsted, L. H. Calcium Carbonate Crystallization in the α-Chitin Matrix of the Shell of Pink Shrimp, Pandalus Borealis, during Frozen Storage. *J. Cryst. Growth* **1997**, *177*, 125–134. https://doi.org/10.1016/S0022-0248(96)00824-X.

(66)    Falini, G.; Weiner, S.; Addadi, L. Chitin-Silk Fibroin Interactions: Relevance to Calcium Carbonate Formation in Invertebrates. *Calcif. Tissue Int.* **2003**, *72*, 548–554. https://doi.org/10.1007/s00223-002-1055-0.

(67)    Weiner, S.; Addadi, L. Crystallization Pathways in Biomineralization. *Annu. Rev. Mater. Res.* **2011**, *41*, 21–40. https://doi.org/10.1159/000324229.

(68)    Noishiki, Y.; Takami, H.; Nishiyama, Y.; Wada, M.; Okada, S.; Kuga, S. Alkali-Induced Conversion of β-Chitin to α-Chitin. *Biomacromolecules* **2003**, *4*, 896–899. https://doi.org/10.1021/bm0257513.

1    (69)   Li, J.; Revol, J.-F.; Marchessault, R. H. Rheological Properties of Aqueous Suspensions of

2            Chitin Crystallites. *J. Colloid Interface Sci.* **1996**, *183*, 365–373.

3    (70)   Harmoudi, H. El; Gaini, L. El; Daoudi, E.; Rhazi, M.; Boughaleb, Y.; Mhammedi, M. A.

4            El; Migalska-zalas, A.; Bakasse, M. Removal of 2,4-D from Aqueous Solutions by

5            Adsorption Processes Using Two Biopolymers : Chitin and Chitosan and Their Optical

6            Properties. *Opt. Mater. (Amst).* **2014**, *36*, 1471–1477.

7    (71)   Muzzarelli, R. A. A. Human Enzymatic Activities Related to the Therapeutic

8            Administration of Chitin Derivatives. *C. Cell. mol. life sci.* **1997**, *53*, 131–140.

9    (72)   Prefecture, S. Dyeing Chitin/Cellulose Composite Fibers with Reactive Dyes. *Text. Res. J.*

10           **2004**, *74* (1), 34–38.

11

2      β-chitin nano-fibrils self-assembly to micro-fibers in a process in which: I) the nucleation is

3      favored in a range around pH 8; II) the polymorphism is conserved and a shrinkage of the unit cell

4      parameter is observed at pH over 11; III) the self-assembly is favored on previously grown fibers

5      that grow preferentially at pH above 8.5 up to a maximum value of thickness.

6



7